Heat transfer in a conjugate heat exchanger with a wavy fin surface

S.F. Tsai, T.W.H. Sheu*, S.M. Lee

Department of Naval Architecture and Ocean Engineering, National Taiwan University, 73 Chou-Shan Road, Taipei, Taiwan 106, Republic of China

Abstract

A three-dimensional computational study on conjugate heat exchangers was conducted. Attention was specifically directed towards studying extended surfaces used to increase heat transfer. The strategy adopted in the present investigation of forced convection in a flow passage was to use the finite volume method. Our implementation incorporated a SIMPLE-based semi-implicit solution algorithm which was applied to working equations formulated within the single-phase catalog. The analysis allowed for marked changes in thermodynamic and flow properties. To justify using the proposed numerical model to simulate this conjugate heat transfer problem, we considered first a heat exchanger with a plane fin simply because experimental data are available for comparison. This validation study was followed by a study of how a newly designed fin pattern can provide increased heat transfer. The efficiency has been judged by considering several aspects, namely the span-averaged pressure drop, Nusselt number and heat flux. To better illuminate the flow and heat transfer characteristics in a flow passage bounded by two fins having wavy geometries, we have plotted solutions in a three-dimensional format. © 1998 Elsevier Science Ltd. All rights reserved.

Nomenclature

B tube pitch
H spacing between plates
L streamwise length of the channel
Nu Nusselt number
p pressure
Pe Peclet number
Pr Prandtl number
$\dot{q}$ heat flux
$\dot{q}_{sp}$ span-averaged heat flux
Re Reynolds number
T temperature [K]
u_i velocity components along i-direction.

Greek symbols
α thermal diffusivity
v kinematic viscosity.

1. Introduction

Conjugate heat transfer finds many applications in daily life. Examples representative of this class of problems are air-conditioning machines, air heaters and power stations. Interest in studying conjugate heat exchangers stems partly from their close relevance to industrial applications and partly from rich physics embedded in the flow passage. It is such practical importance and academic significance of this problem that motivated the present study.

The problem under consideration concerns forced convection heat transfer between a gas and a solid. We are primarily interested in designing a better finned surface in the hope of obtaining a substantial reduction in the size of the heat exchanger. One can achieve this goal by conducting an experimental study or performing a numerical study using the computational fluid dynamics technique. According to Fiebig et al. [1, 2], the current state-of-the-art of experimental calibration does not allow measurement of the conjugate local heat transfer of a finned-tube element. Also, the advent of cost-effective high-speed computation has made possible three-

* Corresponding author. Tel.: 00886 2 23625470; fax: 00886 2 23929885; e-mail: sheu@indy.na.ntu.edu.tw

dimensional fluid dynamics and heat transfer simulations [3]. Numerical analysis has become a tool for providing complements to laboratory experiments and prototyping. With this in mind, we used the computational fluid dynamics technique as an analysis tool to design a wavy-finned surface to enhance heat transfer.

A cylindrical tube, through which one fluid medium flows, and a family of staggered fins, with spacing typically in the range of 300–800 fins m^{-1}, over which air passes constitute the conjugate heat exchanger. There are a number of ways to obtain increased heat transfer coefficients, among which two basic methods have been often referred to. The first method is to devise an appropriate finned shape so that the resulting channel shapes can provide a secondary flow or boundary layer separation that is an aiding factor for a better gas mixing in the flow passage. A further increased heat transfer can be achieved through perforation of the channel, permitting the repeated growth-and-destruction of the boundary layer. The offset strip fin, louvered fin and perforated fin fall into this category. In the past decade, there has been a trend toward using wavy channels to obtain heat transfer enhancement. For these reasons, we considered the wavy fin shape shown in Fig. 1.

This paper begins with an introduction to the working equations and their closure boundary conditions in Section 2. This is followed by a description of the discretization method, the solution algorithm, and a brief introduction to the advective flux discretization scheme. For confident use of the afore-mentioned analysis code to explore the flow and heat transfer complexities in between finned surfaces, we have conducted a validation study on
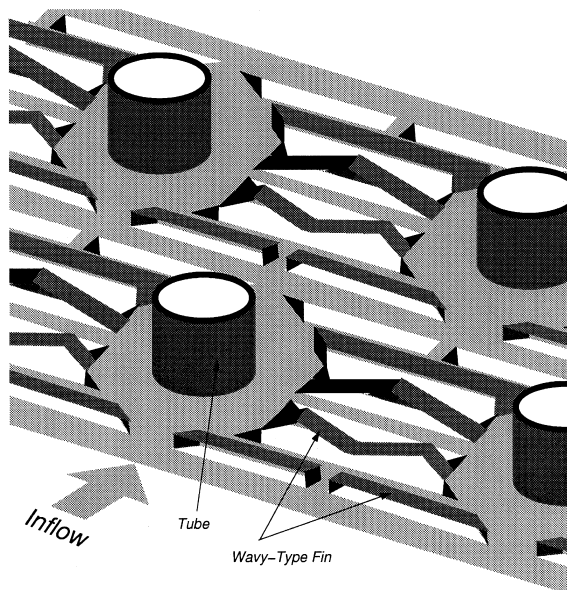
plane fins, as configured in Fig. 2, across which there exist staggered vertical cylindrical tubes. This problem is featured by having a simple geometry and has been experimentally studied by Teco Electronic and Machinery Company in Republic of China (private communication). The available experimental data allow comparison study and, thus, confirmation of the use of computer code developed here. In Section 4, we addressed the numerically predicted flow structure in the channel passage, as described in Section 3, and the temperature distributions on the fin surface. Data obtained from the gas phase were used to produce an animation in order to illuminate some fundamental flow structures that aided the heat transfer enhancement. A manifestation of the increased heat transfer capability over that of the plane fin was demonstrated in terms of span-averaged Nusselt number, heat flux, and pressure drop.

2. Theoretical analysis

2.1. Mathematical model

Under the assumption of zero gravity and other applied forces, working equations capable of rationally describing details of the flow and heat transfer in a conjugated heat exchanger are the following elliptic-parabolic equations:

$$\frac{\partial u_i}{\partial x_i} = 0, \tag{1}$$

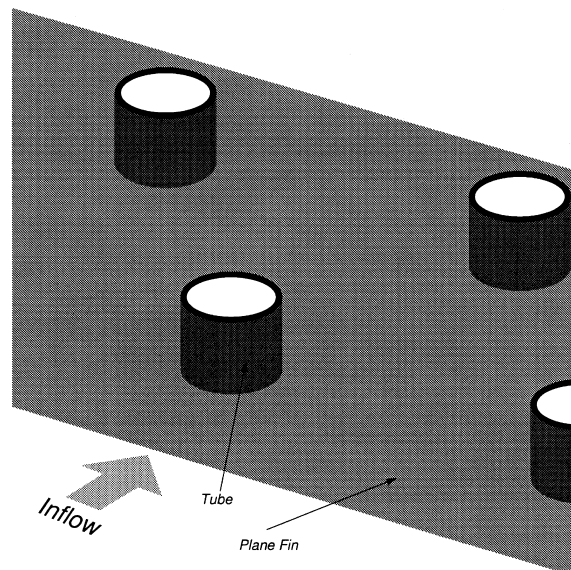Fig. 1. Three-dimensional plot of wavy finned-tube surface.

Fig. 2. Three-dimensional plot of plane finned-tube surface.

$$\frac{\partial u_i}{\partial t} + \frac{\partial}{\partial x_m}(u_m u_i) = -\frac{\partial p}{\partial x_i} + \frac{1}{Re}\frac{\partial^2 u_i}{\partial x_m \partial x_m}. \qquad (2)$$

In the discussion that follows, the Reynolds number is defined as that given in Table 1. As to the air temperature in the flow passage, it is computed from the following conservation of energy equation:

$$\frac{\partial T}{\partial t} + \frac{\partial}{\partial x_m}(u_m T) = \frac{1}{Pe}\frac{\partial^2 T}{\partial x_m \partial x_m}. \qquad (3)$$

The dimensionless dynamical parameter Pe in equation (3) denotes the Peclet number, which is defined as $Pe = Pr \cdot Re$. Here, Pr is the Prandtl number ($Pr = v/\alpha$), where α is the thermal diffusivity. There are several sets of working variables to choose from in the literature. Among these, it is advantageous to employ the primitive-variable formulation for this class of flows simply because this variable setting permits specification of closure boundary and initial conditions [4]. Moreover, these closure conditions are easy to incorporate into the computer code.

2.2. Numerical model

A method which solves the incompressible flow equations (1)–(2) encounters instabilities in situations when advection predominates over diffusion. Spurious oscillations arise in the velocity field, along with prediction

Table 1
Definition of Reynolds numbers and running flow conditions

Re	$\dfrac{\dot{m}D_h}{A_c v} = \dfrac{UD_h}{v}\dfrac{A}{A_c}$
$\dot{m}$	flow rate of air
D_h	hydraulic diameter $(4A_c L)/(A_f + \pi DH/4)$
A_c	minimum flow area of a unit cell
A_f	transfer area for a unit cell
D	tube diameter
L	streamwise length of the channel
H	spacing between plates
A	maximum flow area of a unit cell
U	inlet velocity

Case	Inlet velocity U [m s^{-1}]	Reynolds no.
1	0.81	83
2[1]	1.00	103
3	1.20	124
4[1]	1.50	155
5	1.81	186
6	2.00	206
7[1]	2.50	258

[1] Experimental data are available

inaccuracy due to the so-called false diffusion error, which together grossly pollute the entire domain. To fix this problem, the third-order QUICK upwind scheme [5], implemented on a non-uniform basis, was exploited to model nonlinear advective fluxes. Besides these errors, numerical analysis of this problem suffers from discretization errors stemming from calculation of metric tensors in the use of a one-to-one curvilinear coordinate transformation [6]. Errors of this type are hardly resolvable and cause further deterioration of the prediction accuracy for problems involving highly stretched and distorted meshes. Given that our ultimate goal was to gain insight into the flow structure in the heat exchanger, it was therefore tempting to conduct analyses under simple set of rectangular grids to avoid inaccuracy arising from the coordinate transformation. In this study, grids are carefully designed so that they distribute on surfaces of tubes and fins. Nodal points inside tubes and fins are all blocked off to facilitate the analysis without loss of simulation details.

For an analysis formulated on a velocity-pressure basis, one can apply a grid staggering [7] or a collocating [8] strategy to eliminate node-to-node pressure oscillations. While use of staggered grids for storing working variables leads to programming complexities, we abandoned the collocating grid approach in favor of the first strategy in our segregated approach. The reason for conducting analyses in staggered grids is that proper specification of boundary conditions for the segregated approach conducted in non-staggered grids is still a subject requiring further research. On the cell surface, each primitive variable takes over a node to itself whereas the pressure node is surrounded by velocity nodes. This variable setting permits the use of the finite volume integration method to discretize each conservation equation.

2.3. Solution algorithm

When simulating incompressible fluid flows, it is essential to ensure satisfaction of discrete divergence-free velocities. Therefore, use of the mixed formulation as a model for simulating this type of flow is logical. The accompanying drawback of choosing the mixed formulation as a means to ensure the divergence-free velocity is an involvement of a much larger discrete system. On top of this, the matrix equation has as many zero diagonals as there are continuity equations. The need to avoid excessive demand for computer storage has prompted researchers to consider segregated approaches. In the present paper, the finite volume method was applied to solve Navier–Stokes equations in Cartesian coordinates. The numerical solutions to equations (1)–(3) were obtained as follows. With user-specified initial values as working variables, the continuity and momentum equations (1)–(2) were iteratively solved using the underlying SIMPLE iterative algorithm [7]. When the

residuals in the flow equations reached their user-specified tolerances, the energy equation (3) was solved using the computed convergent velocities.

3. Problem description

Referring to Fig. 3, the physical problem under consideration is that of a laminar flow through a bundle of parallel staggered cylinder pipes. The problem, configured as the plane-fin-tube configuration shown in Fig. 2, was used for validation purposes. The flow pattern in this finned-tube heat exchanger can be fairly complex due to the three-dimensional nature of the flow separation and helixes. There are several geometric variables that may appreciably affect the heat transfer coefficient. For this study, the presence of cylinder tubes which were arranged in a triangular form, as a result of connecting the circles of the three adjacent cylinders, was the main cause of yielding a greatly altered flow structure in the passage. For this study, no attempt has been made to study the effect of geometric parameters on the heat transfer characteristics. The fin pitch, fin height and fin thickness remained fixed throughout this study.

Close examination of the horizontal array of staggered pipes, shown in Fig. 3, reveals that it is possible to apply a periodic condition at the boundaries shown in Fig. 4. This facilitated the analysis in the sense that the computational domain, scaled by $2L:B:D = 25.5:20.4:1.4$, has been dramatically reduced. At the inlet plane, which was upstream of the leading edge of the fin plate at a distance of 4.5 mm, the velocity was kept constant. The temperature prescribed there was also kept constant at $T = T_0 = 300°$K. To save disk space, the outlet plane was truncated at a plane which was sufficiently distant from the trailing edge of the fin plate. On physical grounds, the streamwise gradients were set to zero at the synthetic outlet:
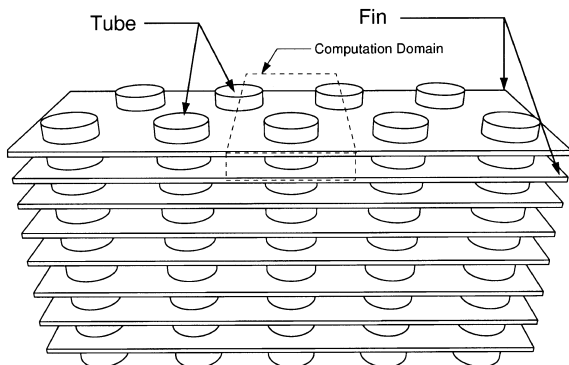

Fig. 3. Schematic of two-row fin and tube heat exchanger configuration. Analysis is conducted in dotted area due to flow periodicity.
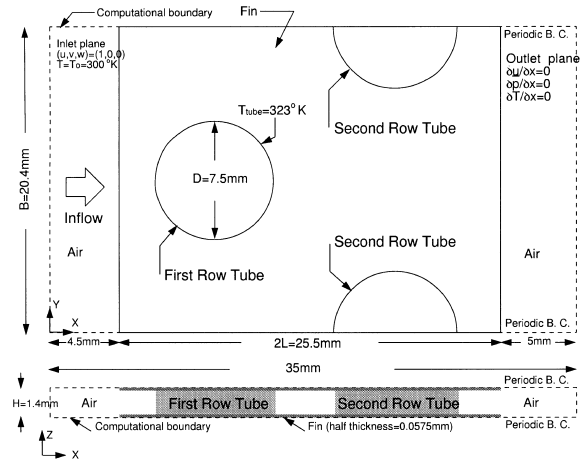

Fig. 4. A finned-tube element as module geometry for the investigation. Included in this figure are also prescribed boundary conditions.

$$\frac{\partial \underline{u}}{\partial x} = \frac{\partial p}{\partial x} = \frac{\partial T}{\partial x} = 0. \tag{4}$$

While use of the above zero gradient outlet boundary condition provides close agreement with the experimental data for the plane fin heat exchanger as discussed in Section 4, the application of this set of boundary conditions to simulate problems involving more complex geometries warrants a further detailed investigation. Besides the no-slip walls where zero velocity components applied, the rest of the boundaries were classified as periodic boundaries where the following boundary conditions hold:

$$\underline{u}(x, 0, z) = \underline{u}(x, B, z), \quad \underline{u}(x, y, 0) = \underline{u}(x, y, H);$$

$$T(x, 0, z) = T(x, B, z), \quad T(x, y, 0) = T(x, y, H). \tag{5}$$

On the vertical tube where no-slip conditions held, the temperature was kept at a constant value of 323 K. With the knowledge that the velocity and thermal boundary layers could develop over the no-slip wall, grids had to be well-stretched to capture the high-gradient velocity and thermal boundary layers. Throughout this study, the flow passage was covered with non-uniform grids with a resolution of $142 \times 84 \times 40$ for the case of plane fins while $142 \times 84 \times 54$ was the resolution for the wavy fins. According to the inlet air velocities and the chosen reference length, namely, the height H behind the two fin plates, the Reynolds numbers under consideration took values summarized in Table 1.

4. Results and discussion

It is the opinion of the authors that validation of the developed computer code is a necessary step in the

numerical simulation of heat transfer in a finned-tube heat exchanger. To this end, two tasks were conducted a priori. In the first place, a validation study was conducted for the case which was amenable to analytic solutions. We cast prediction errors for cases with different mesh sizes in L_2-error norms. These norms enabled us to estimate the rate of convergence for velocities and pressure. For brevity, the analytic validation of the computer code employed in this article has been given elsewhere. Interested readers are referred to [9] for additional details.

We then proceeded to make a comparison of the experimental and numerical data. The discussion of results was focused on air with $Pr = 0.7$ and inlet velocity $u = 1.2$ m s^{-1}. By definition, as given in Table 1, the Reynolds number under the circumstances falls into the range of daily encountered finned-tube heat exchangers. For this study the pressure drop and the heat transfer rate through the plane finned-tube heat exchanger were chosen for comparison. As Figs 5–6 show, agreement between the measured and computed data was acceptable. With this
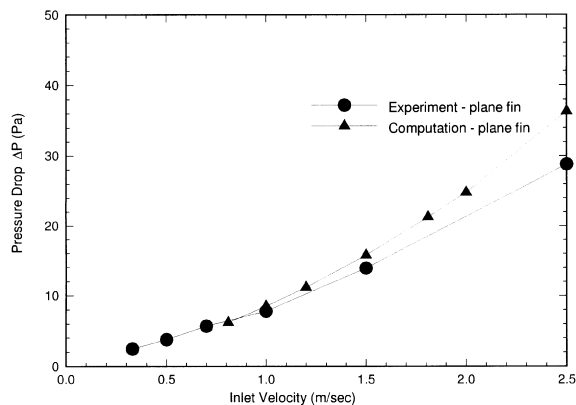
Fig. 5. A comparison of computed and measured pressure drops against inlet velocities summarized in Table 1.
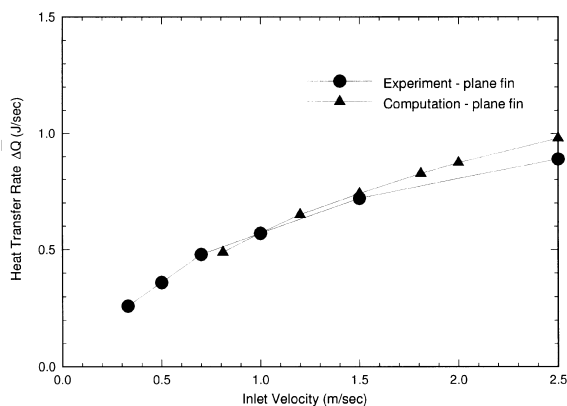

Fig. 6. A comparison of computed and measured heat transfer rates against inlet velocities summarized in Table 1.

success in conducting analytic and experimental validation, we had sufficient confidence to explore the physics of the air flow in the finned-tube passage of heat exchangers.

To begin with, we plotted in Fig. 7 the heat flux distribution on the plane fin surface for the case of $Re = 124$. Revealed from this figure is that the largest value of $\dot{q}$ appeared in regions adjacent to the leading edge of the finned plate. The reason for such a local maximum value of $\dot{q}$ was the flow development, which aided convective heat transfer at the leading edge. In regions other than the leading edge, larger heat fluxes were also found in regions just upstream of two rows of tubes. In contrast, the reason for the high value of $\dot{q}$ observed in the upstream part of the tube was the greater exchange of bulk fluids with fluids adjacent to the wall in the horseshoe vortex shown in Fig. 8. Another reason for the local heat transfer enhancement was the high temperature on the fin and the low bulk temperature. We plotted in Fig. 9 the heat flux distribution on the wavy fin configured in Fig. 1. A trend similar to that found in the plane fin was observed. The value of $\dot{q}$ reaches its maximum as the tube was approached.

We then computed some span-averaged quantities of physical significance. Figure 10 shows the span-averaged Nusselt number in the streamwise direction for the plane fin under the inlet directions tabulated in Table 1. Clearly revealed in this figure is an abrupt increase of Nu which occurs in front of the tube. This increase was the result of the horseshoe vortex formation. There was also a gradual drop of Nu from its maximum value at the leading edge due to the boundary layer development. For the sake of completeness, we plotted the span-averaged $\dot{q}_{sp}$ in Fig. 11 for the wavy-type finned-tube exchanger.

Determining the amount of pressure drop is the key to success of heat exchanger design. This led us to plot the pressure drop for the wavy fin. As shown in Fig. 12, pressure drops for both fins were mainly found in the range where cylindrical tubes were mounted while a comparatively mild pressure drop was observed behind and in front of the tube. The reason for the pressure drop was the established form drag of the tube.

To illuminate the physics of fluid in the flow passage of finned-tube heat exchanger, it is useful to plot the velocity vectors. Since the physical domain under investigation was restricted to a narrow region in which circular tubes were staggered, the flow structure was definitely three-dimensional. This was in strong contrast to the case which involves a domain of infinite lengths. In addition to the circular cylinders, perforated fins added further complications to the flow because of the termination of boundary layer development. This, together with the stagnant nature of the flow in regions adjacent to the perforated fin surface, caused a secondary flow pattern at transverse planes shown in Fig. 13. For better representation of the three-dimensional nature of the
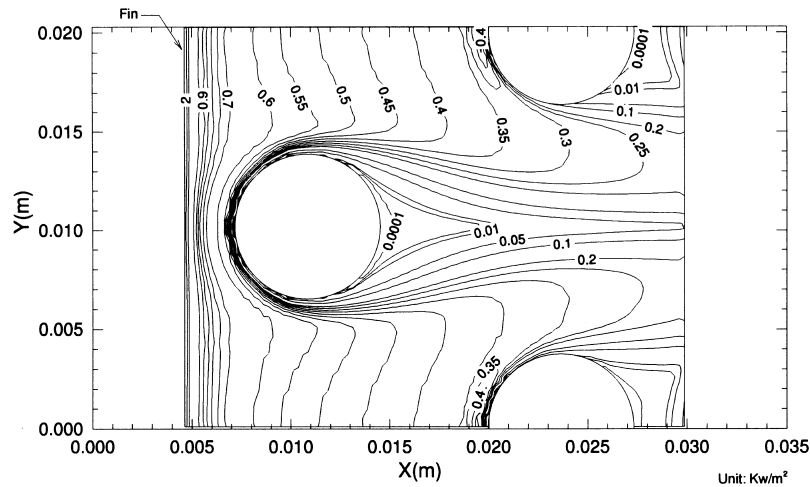
Fig. 7. A contour plot of heat flux $\dot{q}$ on the plane fin for the case of $Re = 124$ (or inlet velocity is 1.2 m s^{-1}).

flow, we traced particles which were seeded at appropriate locations. Particles were entrained by the longitudinal vortices which were generated by the perforated fin. The formation of longitudinal vortices, as shown in Fig. 14, was believed to be the result of the pressure difference exerted between the pressure and suction sides of the perforated fin. This observation was indicated earlier by Biswas et al. [10]. It was this local formation of longitudinal vortices that caused the spanwise particle motion. In the presence of such spanwise mixing, an increase in the heat transfer would be expected. Figure 15 shows a heat transfer enhancement, as compared with the case without fin perforation.

The heat transfer enhancement was also attributable to the spiralling nature of the horseshoe vortex which formed in front of the tube. The center of the horseshoe vortex was regarded as the critical point. By definition, particles adjacent to the rotating center of the horseshoe vortex spiralled toward this point. This aided mixing of the fluid flows and, in turn, caused the heat transfer enhancement. To confirm this finding, we have prepared an animation displaying a sequence of temperature contours at the (x, y) plane. Through this animation, one can clearly observe that larger temperature gradient was found to appear in regions where a horseshoe vortex was present. A collection of horseshoe vortex centers formed a vortical core line, as shown in Fig. 16, revealing that particles near the vortical core line were entrained towards the vortex center. Revealed also from this figure

is that particles proceeded downstream in a three-dimensional spiralling fashion.

5. Concluding remarks

In this study, we have provided computational evidence for the rational use of wavy-type extended fin surfaces as a means to enhance heat transfer in a finned-tube heat exchanger element. The motivation behind perforating fin surfaces was rooted in the fact that perforation can cause the development and destruction of the boundary layer. Besides this, the formation of a horseshoe vortex which wrapped the cylinder surface aided flow mixing and, thus, increased heat transfer. This study also explored in depth the flow physics from the topological study of the computed three-dimensional data and the animation display of flow and thermal fields.
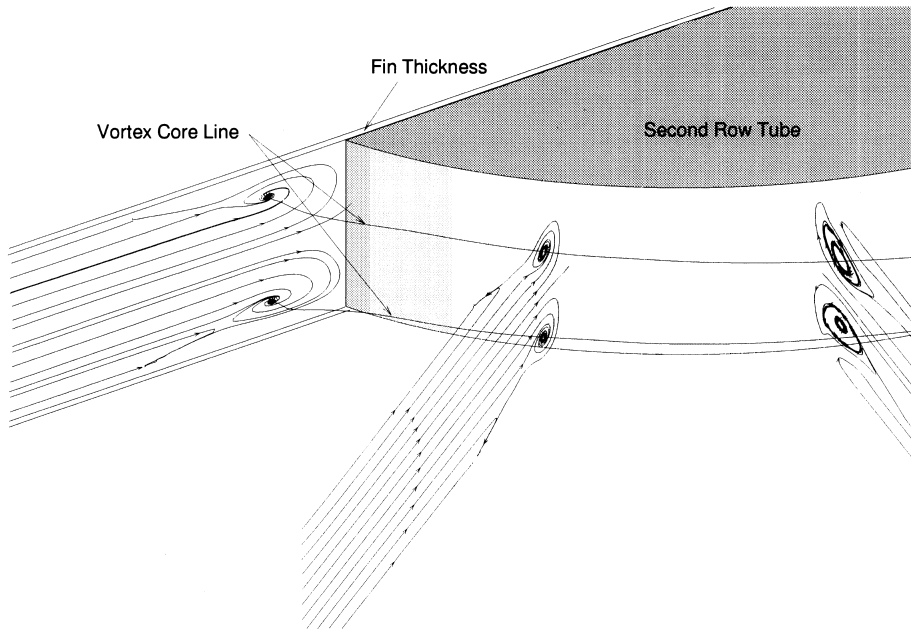
Fig. 8. An illustration of vortical core line in front of the second-row of the plane finned-tube heat exchanger cylinder.
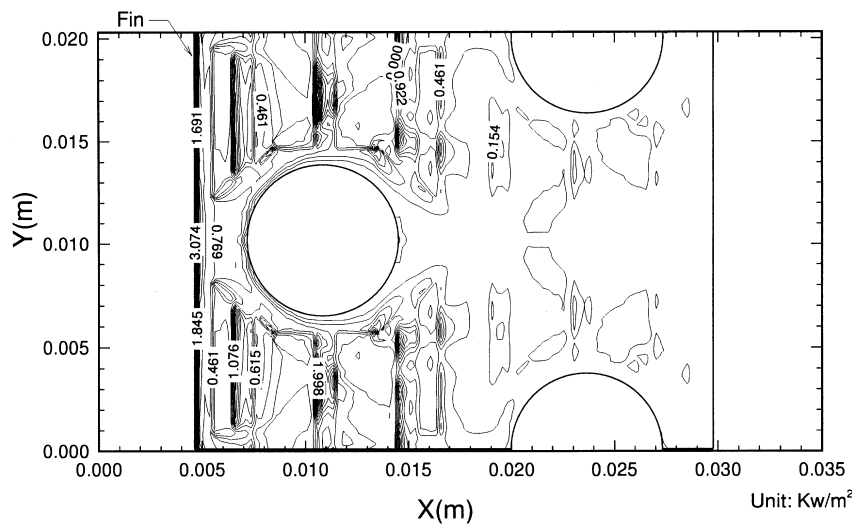

Fig. 9. Contour of heat fluxes on the $z = 0$ surface of wavy-type heat exchanger.
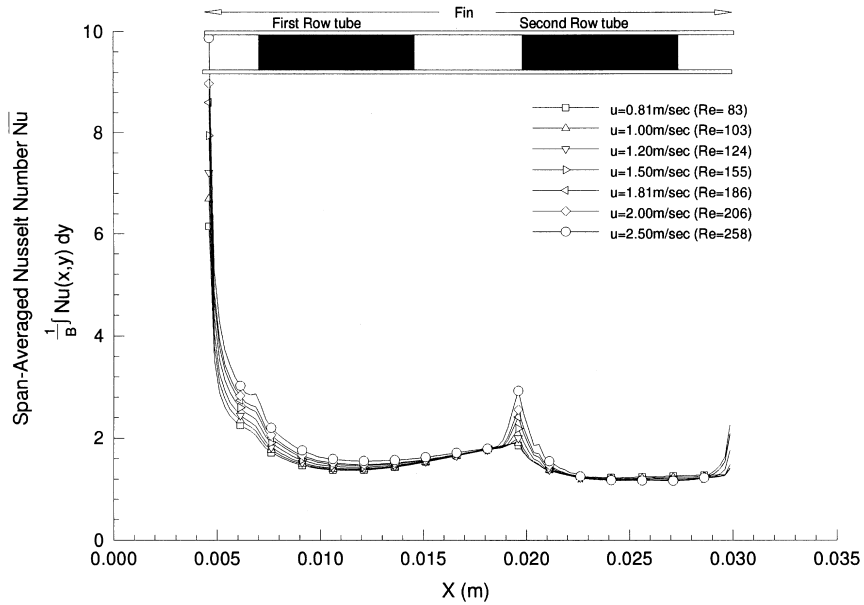
Fig. 10. Span-averaged Nusselt numbers in the streamwise direction as a function of Reynolds numbers for the plane fin under investigation.
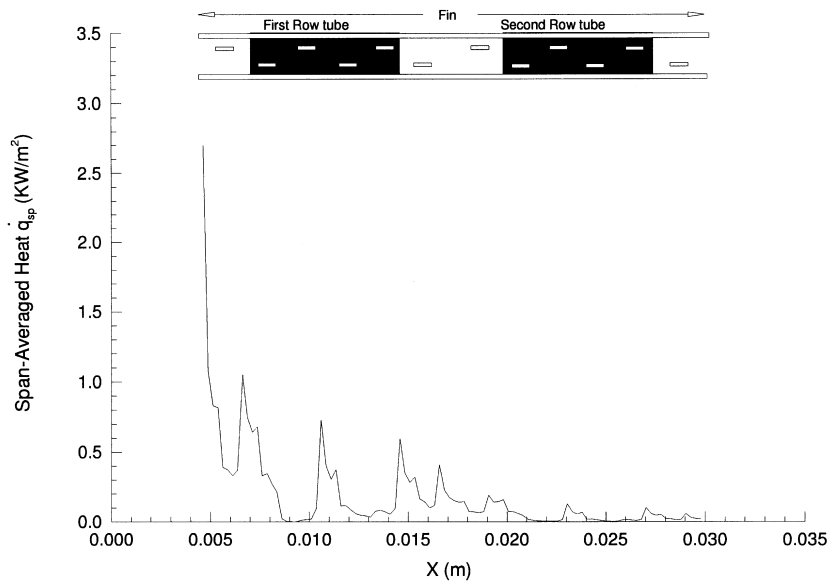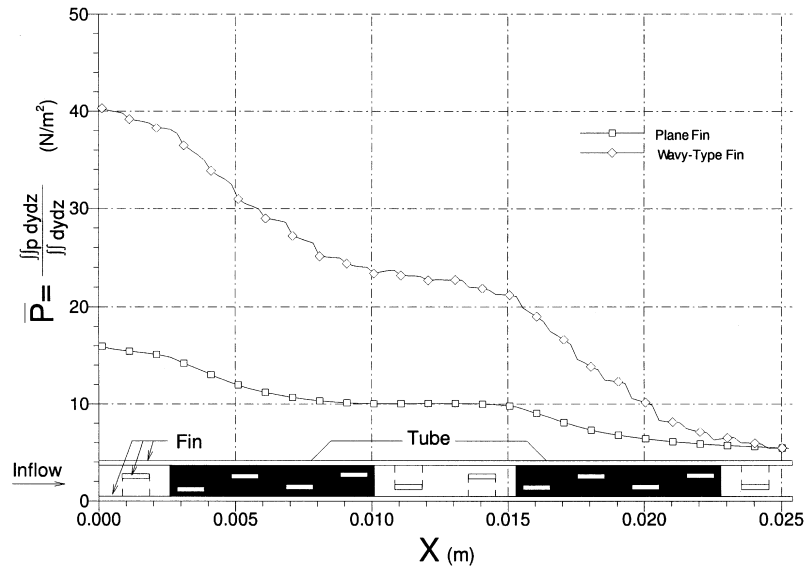

Fig. 11. Span-averaged $\dot{q}_{sp}$ in the streamwise direction as a function of Reynolds numbers for the wavy-type fin under investigation.

Fig. 12. Averaged pressure distribution in the streamwise direction for plane and wavy-type fins.
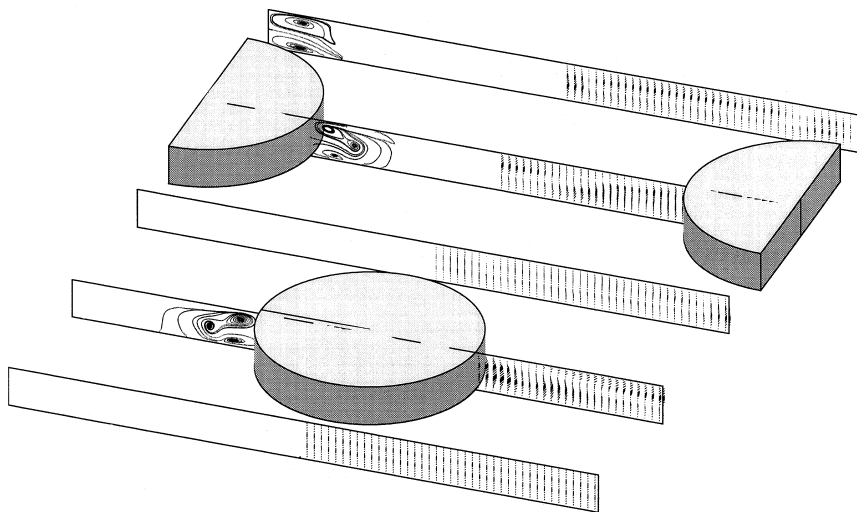

Fig. 13. Vector plots and streamline contours at *y–z* planes to illustrate the secondary flow formation.
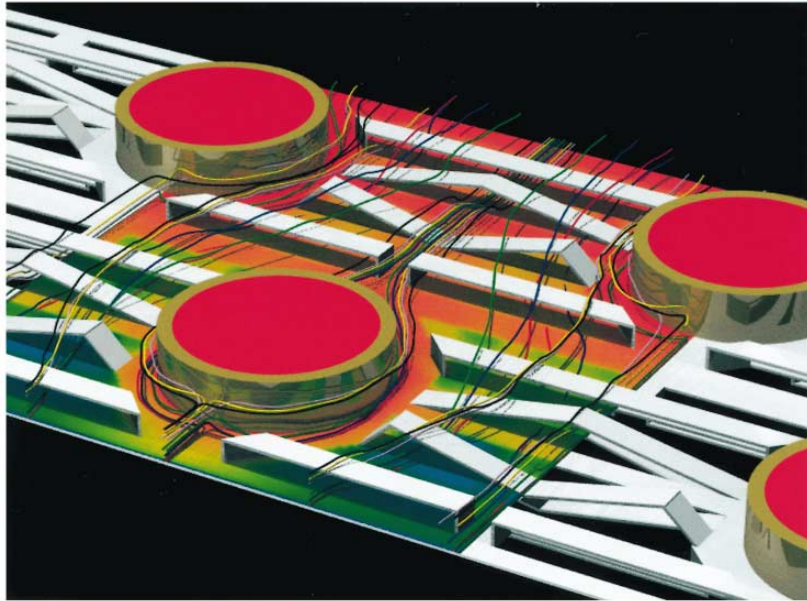
Fig. 14. Three-dimensional particle tracks in the flow over a heat exchanger shown in Fig. 1.
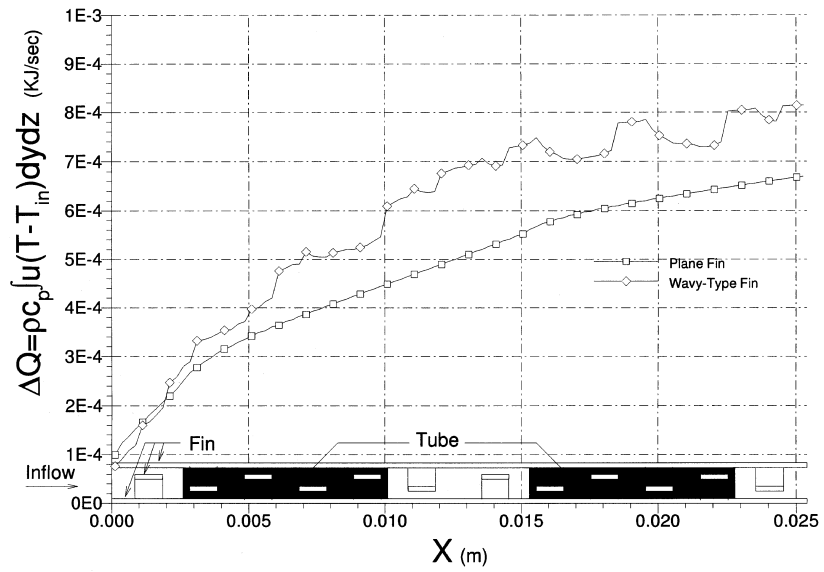

Fig. 15. Span-averaged heat transfer in the streamwise direction for the two fin surfaces investigated.
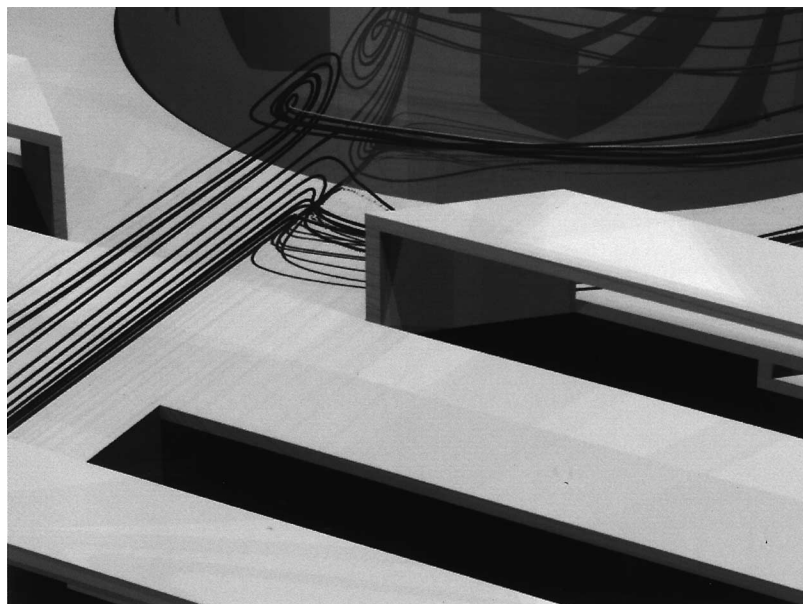
Fig. 16. An illustration of vortical core line in front of the second-row of the wavy-type finned-tube heat exchanger cylinder.

References

[1] M. Fiebig, A. Grosse-Gorgemann, Y. Chen, N.K. Mitra, Conjugate heat transfer of a finned tube Part A: heat transfer behavior and occurrence of heat transfer reversal, Num. Heat Transfer, Part A 28 (1995) 133–146.

[2] M. Fiebig, Y. Chen, A. Grosse-Gorgemann, N.K. Mitra, Conjugate heat transfer of a finned tube Part B: heat transfer augmentation and avoidance of heat transfer reversal by longitudinal vortex generators, Num. Heat Transfer, Part A 28 (1995) 147–155.

[3] A. Valencia, M. Fiebig, N.K. Mitra, Heat transfer enhancement by longitudinal vortices in a fin-tube heat exchanger element with flat tubes, ASME J. Heat Transfer 118 (1996) 209–211.

[4] O.A. Ladyzhenskaya, Mathematical Problems in the Dynamics of a Viscous Incompressible Flow, Gordon and Breach, New York, 1963.

[5] B.P. Leonard, A stable and accurate convective modelling procedure based on quadratic upstream interpolation, Comput. Methods Appl. Mech. Engrg. 19 (1979) 59–98.

[6] W.H. Sheu, S.M. Lee, A segregated solution algorithm for incompressible flows in general coordinates, Int. J. Numer. Methods Fluids 22 (1996) 1–34.

[7] S.V. Patankar, Numerical Heat Transfer and Fluid Flow, Hemisphere, Washington, DC, 1980.

[8] S. Abdallah, Numerical solution for the incompressible Navier–Stokes equations in primitive variables using a non-staggered grid, II, J. Comp. Phys. 70 (1987) 193–202.

[9] T.P. Chiang, R.R. Hwang, W.H. Sheu, Finite volume analysis of spiral motion in a rectangular lid-driven cavity, Int. J. Numer. Methods Fluids 23 (1996) 1–22.

[10] G. Biswas, N.K. Mitra, M. Fiebig, Heat transfer enhancement in fin-tube heat exchangers by winglet type vortex generators, Int. J. Heat Mass Transfer 37 (1994) 283–291.